CSIRO PUBLISHING

Australian Journal of Physics

Volume 52, 1999

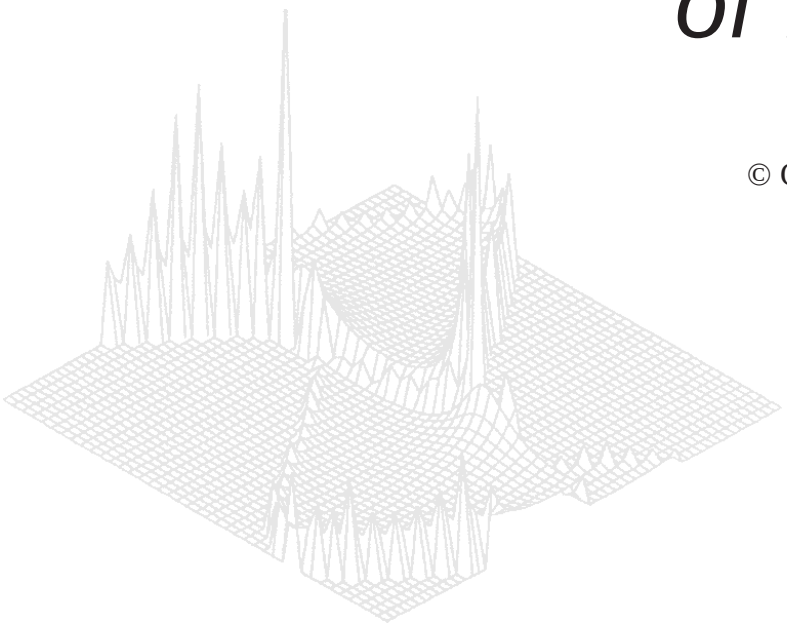

A journal for the publication of
original research in all branches of physics

www.publish.csiro.au/journals/ajp

All enquiries and manuscripts should be directed to
Australian Journal of Physics
CSIRO PUBLISHING
PO Box 1139 (150 Oxford St)
Collingwood Telephone: 61 3 9662 7626
Vic. 3066 Facsimile: 61 3 9662 7611
Australia Email: peter.robertson@publish.csiro.au

Published by **CSIRO** PUBLISHING
for CSIRO Australia and
the Australian Academy of Science

Aust. J. Phys., 1999, **52**, 323–39

Threshold Behaviour of (e, 2e) Reactions in Classical and Quantum Mechanics*

H. Friedrich,[A] *W. Ihra*[B] *and P. Meerwald*[A]

[A]Physik-Department, Technische Universität München,
85747 Garching, Germany.
[B]Max-Planck-Institut für Physik Komplexer Systeme,
01187 Dresden, Germany.

Abstract

Electron impact ionisation of one-electron atoms or ions is well described in the near threshold region by Wannier's theory based on estimating the classical phase space available to two outgoing electrons in the Coulomb field of the residual ion. The relation between classical dynamics and quantum mechanics in the near threshold region becomes more complicated and interesting in 'non-Wannier situations', where classical ionisation is either strictly forbidden or strongly inhibited. This paper focusses on two examples of such situations, which have been receiving increasing attention in recent years, namely the *s*-wave model and the case where the exponent in Wannier's law diverges.

1. Introduction

An accurate description of the ionisation of a ground state hydrogen atom by electron impact,

$$\mathrm{e}^- + \mathrm{H} \longrightarrow \mathrm{e}^- + \mathrm{e}^- + \mathrm{H}^+ , \tag{1}$$

has occupied atomic physicists for half a century. At energies somewhat above the ionisation threshold, $E = 0$, the correct reproduction of the observed total ionisation cross section $\sigma(E)$ (Shah *et al.* 1987) proved very difficult, and standard approximation techniques as well as large scale numerical calculations were unsuccessful for a long time. The breakthrough came when Bray and Stelbovics (1993) applied their 'convergent close coupling' (CCC) technique to calculate $\sigma(E)$ *ab initio*. The success of their calculation and also the failure of other elaborate efforts is demonstrated in Fig. 1. Another focus of attention has been the behaviour of $\sigma(E)$ in the immediate vicinity of the threshold. Wannier (1953) investigated how the volume of classical phase space allowing the reaction (1) grew with increasing energy and thus derived his famous threshold law,

$$\sigma(E) \propto E^{\nu_{\mathrm{W}}} , \qquad \nu_{\mathrm{W}} = \tfrac{1}{4}\left(\sqrt{\frac{100Z-9}{4Z-1}} - 1\right). \tag{2}$$

* Refereed paper based on a contribution to the Australia–Germany Workshop on Electron Correlations held in Fremantle, Western Australia, on 1–6 October 1998.

 10.1071/PH98091 0004-9506/99/030323$10.00

The explicit form (2) of the threshold law refers to a system with an infinitely heavy nucleus of charge Z and two outgoing electrons, and we shall, for simplicity confine the discussion to these conditions. Generalisations of Wannier's classical theory have been formulated to describe the general three-body Coulomb problem and, quite recently, for the break-up of a system into any number of particles interacting exclusively via Coulomb forces (Kuchiev and Ostrovsky 1998). Many authors have formulated quantum mechanical theories of near threshold ionisation involving various degrees of classical or semiclassical assumptions (Rau 1971; Feagin 1984; Macek and Ovchinnikov 1996) and, with some exceptions (Temkin 1991), most such investigations support Wannier's result.

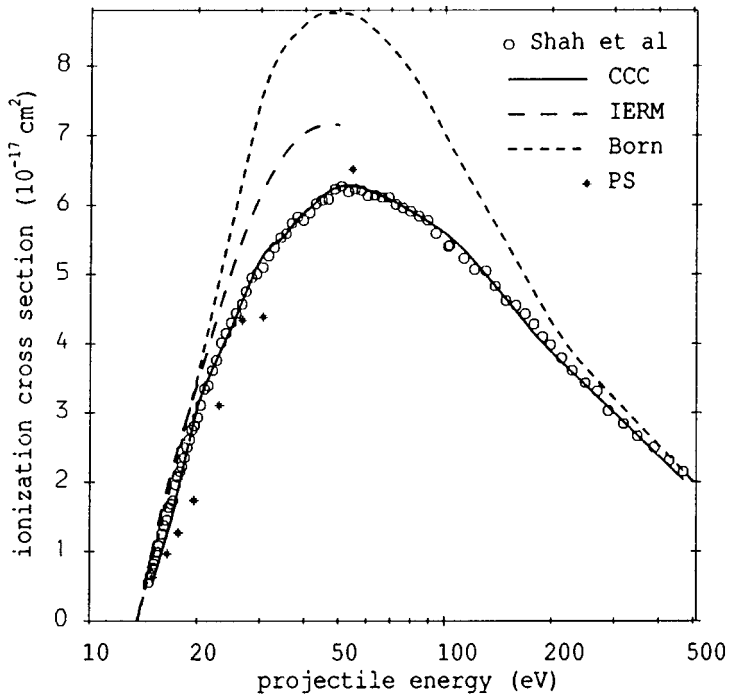

Fig. 1. Total ionisation cross sections for the reaction (1). The open circles are the experimental results from Shah *et al.* (1987) and the solid line is the result of the *ab initio* calculation of Bray and Stelbovics. The crosses and the long-dashed line show the results of other elaborate theoretical calculations, published in 1979 and 1990 respectively. [From Bray and Stelbovics (1993).]

Simple classical phase space arguments are not so useful in 'non-Wannier' situations which occur, e.g., when ionisation is classically either strictly forbidden or strongly inhibited in the near threshold region. Examples are the s-wave model and the situation where the charge of the light particles (the 'electrons') is four times the charge of the heavy particle (the 'residual ion'), which effectively corresponds to a nuclear charge $Z = \frac{1}{4}$. The aim of this paper is to draw attention to these non-Wannier situations where the relation between classical and quantum mechanics is a bit more subtle.

All systems discussed consist of particles interacting exclusively via Coulomb forces, and simple scaling rules apply in such systems with homogeneous potentials. These scaling rules allow an unambiguous definition of the semiclassical limit as explained in Section 2. Section 3 briefly reviews the collinear model, where the classical approximation and Wannier's theory work well, and the subsequent two sections discuss examples of non-Wannier systems where the traditional Wannier theory breaks down.

2. Semiclassical Limit

Consider a physical system with any number f of degrees of freedom, whose kinetic energy is $T = \sum_{i=1}^{f} p_i^2/2m_i$ and whose potential energy is described by a homogeneous function $V(x_1, \ldots x_f)$ of the coordinates,

$$V(\xi x_1, \ldots, \xi x_f) = \xi^d V(x_1, \ldots, x_f)\,. \tag{3}$$

If the trajectory $(x_i(t), p_i(t))$ describes the classical motion at the (conserved) total energy E, then the scaled trajectory $(\xi x_i, \xi^{d/2} p_i)$ describes mechanically similar motion at the energy $E' = \xi^d E$ (Landau and Lifshitz 1971). Hence the classical dynamics depends only on the sign of E and not on its magnitude. The quantum mechanics obtained by quantising the classical dynamics with Planck's constant $\hbar$ at energy E is equivalent to that obtained by quantising the scaled dynamics at energy E' with an *effective Planck's constant* $\hbar'$ (Friedrich 1998*a*; see also Sect 5·3·4 in Friedrich 1998*b*):

$$\hbar' = \xi^{1+d/2}\hbar = \left(\frac{E'}{E}\right)^{1/d+1/2} \hbar\,. \tag{4}$$

For a given (constant) energy E' in the scaled system, the semiclassical limit corresponds to $\hbar' \to 0$. For the equivalent quantum mechanics in the physical system ($\hbar$ constant), this corresponds to $(E'/E)^{1/d+1/2} \to 0$. The semiclassical limit in a homogeneous potential of degree d is thus reached for

$$|E| \to \infty \quad \text{if} \quad d > 0 \text{ or } d < -2\,, \tag{5}$$

but it is reached for

$$|E| \to 0 \quad \text{if} \quad -2 < d < 0\,. \tag{6}$$

For all systems of particles interacting exclusively via Coulomb forces, the potential energy is homogeneous of degree $d = -1$, so the semiclassical limit is not at high energies but for vanishing total energy of the system. This applies to all atoms, ions and molecules, as long as the atomic nuclei are treated as point particles and nonclassical interactions such as those involving spin are ignored.

In a collision process, the initial state consists of a projectile and a target which are well separated. The initial binding energy E_b of the target is positive for a stable target and is, e.g., equal to $Z^2/2n^2$ (in atomic units) for a one-electron atom (or ion) of nuclear charge Z in an eigenstate of principal quantum number n.

The incoming kinetic energy E_{inc} of relative motion of the projectile and the initial binding energy E_{b} of the target combine to make up the total energy $E = E_{\mathrm{inc}} - E_{\mathrm{b}}$. Choosing a particular initial binding energy E_{b} defines a reference energy and the classical dynamics is not independent of E for fixed E_{b}. However, due to the scaling properties in the homogeneous potential, the classical dynamics depends not on E and E_{b} independently, but only on the ratio E/E_{b}, which we shall call the *scaled energy* ε:

$$\varepsilon = E/E_{\mathrm{b}}\,. \tag{7}$$

This applies to all observables calculated in the classical framework, e.g. to the (differential or integrated) classical ionisation cross section:

$$\sigma_{\mathrm{cl}}(E, E_{\mathrm{b}}) = \sigma_{\mathrm{cl}}(\varepsilon)\,. \tag{8}$$

The threshold behaviour of the classical ionisation cross section is the behaviour of the function $\sigma_{\mathrm{cl}}(\varepsilon)$ as $\varepsilon \to 0$.

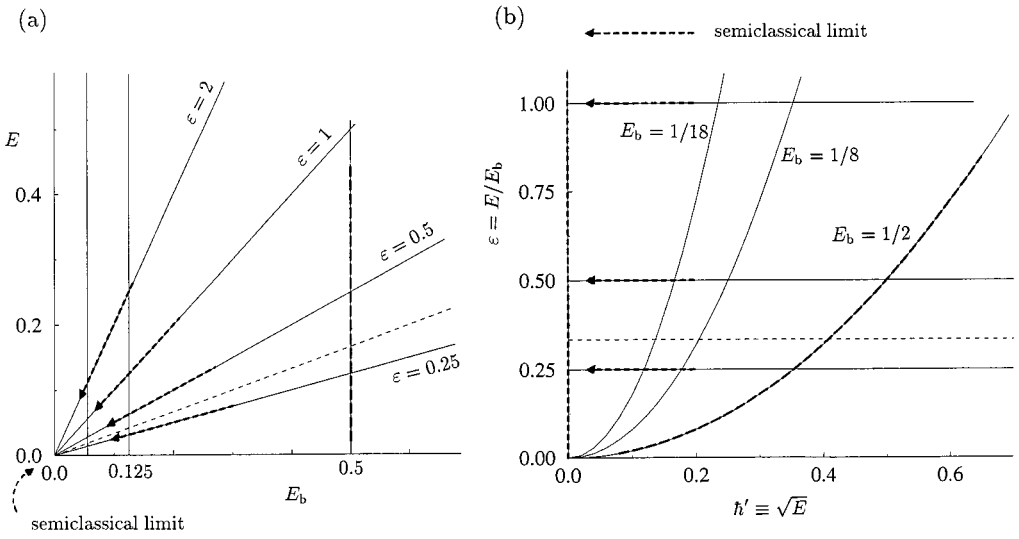

Fig. 2. (*a*) Plane spanned by the total energy E and the initial target binding energy E_{b} as determining variables of a projectile–target collision. If the potential is homogeneous, the classical dynamics of the collision depends only on the scaled energy, $\varepsilon = E/E_{\mathrm{b}}$, and is invariant along the lines of constant ε, shown as rays from the origin. For a Coulombic potential, the semiclassical limit is reached by approaching the origin on one of these rays. (*b*) The same plane spanned by the alternate variables ε, which determines the classical dynamics, and $\sqrt{E}$, which plays the role of an effective Planck constant $\hbar'$ and determines how close we are to the semiclassical limit. The semiclassical limit is now reached by approaching the ordinate on horizontal lines. Approaching the threshold $E \to 0$ for a fixed initial binding energy E_{b} corresponds to approaching the origin on a half-parabola, $\varepsilon = (\hbar')^2/E_{\mathrm{b}}$. In each part of the figure, the thick long dashed line marks the range covered by the classical calculation shown in Fig. 4, see Section 3. In the area bounded by the abscissa and the thin dashed line, ionisation of hydrogen is classically forbidden in the *s*-wave model, see Section 4.

The quantum mechanical (differential or integrated) ionisation cross section $\sigma_{\rm qm}(E, E_{\rm b})$ depends on both variables E and $E_{\rm b}$, which span the plane shown in Fig. 2*a*. Alternate variables are the scaled energy (7), which determines the classical dynamics, and the effective Planck constant (4), which determines how close we are to the semiclassical limit, see Fig. 2*b*. Remembering that $d = -1$ and choosing E' in (4) to be unity we have ($\hbar = 1$)

$$\hbar' = \sqrt{E}\,. \tag{9}$$

The semiclassical limit at a given scaled energy ε is reached for $\hbar' \to 0$ implying $E \to 0$ (and $E_{\rm b} \to 0$). This corresponds to approaching the origin on one of the rays in Fig. 2*a* or to approaching the ordinate horizontally in Fig. 2*b*.

In order to reach the semiclassical limit, experiments or quantum mechanical calculations should be performed at constant values of the scaled energy (7). This is analogous to the technique of 'scaled energy spectroscopy', which has become a widely used tool in the analysis of atoms in external fields (Friedrich 1998*a*, 1998*b*; Friedrich and Eckhardt 1997; Schmelcher and Schweizer 1998). In the semiclassical limit, $\hbar' \to 0$, the quantum mechanical ionisation cross section will converge to a generally finite value given by the classical (semiclassical) calculation. This is true for all values of the scaled energy (7), in particular near threshold, so the classical (semiclassical) threshold behaviour should be reproduced if we proceed in this way.

However, most experimental (and theoretical) investigations of near threshold ionisation study the behaviour of $\sigma_{\rm qm}(E, E_{\rm b})$ for fixed initial binding energy $E_{\rm b}$ and small total energy, $E \to 0$. This corresponds to approaching the abscissa on a vertical line in Fig. 2*a* or to approaching the origin on one of the half-parabolas,

$$\varepsilon = \frac{(\hbar')^2}{E_{\rm b}}\,, \tag{10}$$

in Fig. 2*b*.

Even if we assume that the quantum mechanical ionisation cross section $\sigma_{\rm qm}(E, E_{\rm b}) \equiv \sigma_{\rm qm}(\varepsilon, \hbar')$ is well approximated by the classical expression $\sigma_{\rm cl}(\varepsilon)$ in a region around the origin in Fig. 2*b*, the explicit form of the threshold behaviour can depend on how we approach the origin. If $\sigma_{\rm cl}(\varepsilon)$ behaves as a power of ε near $\varepsilon = 0$, then the $E_{\rm b}$-dependence of the ionisation cross section simply factors out,

$$\sigma_{\rm cl}(\varepsilon) \propto \varepsilon^{\nu} \Longrightarrow \sigma_{\rm qm}(E, E_{\rm b}) \approx \sigma_{\rm cl}(E/E_{\rm b}) \propto E_{\rm b}^{-\nu} \times E^{\nu}\,, \tag{11}$$

and the quantum mechanical threshold behaviour of the cross section for any fixed initial binding energy $E_{\rm b}$ is given by the same power law; the dependence on the initial binding energy merely affects the constant of proportionality. This is not the case for a more general behaviour of $\sigma_{\rm cl}$. Take for example the exponentially damped case,

$$\sigma_{\rm cl}(\varepsilon) \propto {\rm e}^{-a/\varepsilon^{\nu}} \Longrightarrow \sigma_{\rm qm}(E, E_{\rm b}) \approx \sigma_{\rm cl}(E/E_{\rm b}) \propto \left({\rm e}^{-a/E^{\nu}}\right)^{E_{\rm b}^{\nu}}\,. \tag{12}$$

Changing E_b now affects the whole shape of the cross section as function of energy, and not just a proportionality constant. The appropriate threshold law does not depend only on whether ionisation is described classically or quantum mechanically. It depends crucially on how the threshold is approached. If the cross section is calculated for fixed scaled energy E/E_b, it should approach the classical (semiclassical) result near threshold, $E \equiv (\hbar')^2 \to 0$. However, the limiting behaviour of $\sigma_\mathrm{qm}(E, E_\mathrm{b})$ along one of the half-parabolas (E_b constant, $E \to 0$) need not be the same as along the ordinate ($\hbar' = 0$, $\varepsilon \to 0$).

3. The Collinear Model

The electron impact ionisation of a one-electron atom involves two electrons moving in the Coulomb field of the nucleus. The important coordinates are the separations r_1, r_2 of the two electrons from the nucleus and the angle θ between the corresponding radius vectors. Directly at threshold, the two electrons can only escape if they asymptotically approach the 'Wannier configuration', $r_1 = r_2$, $\theta = \pi$. The classical motion in this configuration is stable against bending away from the collinear configuration $\theta = \pi$, but unstable against deviations in the direction $r_1 \neq r_2$. This makes it meaningful to study the classical motion of the collinear configuration, in which both electrons are on opposite sides of the nucleus ($\theta = \pi$), as has been done in considerable detail by Rost (1994, 1998).

The model has two degrees of freedom, r_1 and r_2, and is described by the potential energy

$$V_\mathrm{COL}(r_1, r_2) = -\frac{Z}{r_1} - \frac{Z}{r_2} + \frac{1}{r_1 + r_2}\,, \tag{13}$$

which is illustrated for the case of a hydrogen target ($Z = 1$) in Fig. 3. In the initial state, the inner electron oscillates on a linear Kepler orbit corresponding to the hydrogen ground state ($E_\mathrm{b} = \frac{1}{2}$), while the outer electron approaches from $+\infty$ with asymptotic kinetic energy $E + \frac{1}{2}$, $E \geq 0$. In this one-dimensional world, reaction cross sections are replaced by dimensionless probabilities, and the probability for ionisation is given by the fraction of ionising trajectories.

The classical ionisation probabilities, integrated over the energy distribution of the two outgoing electrons, were calculated by Rost (1994, 1998) and are shown in Fig. 4; they were scaled by a constant factor to fit the experimental data (McGowan and Clarke 1968) at one energy (5·84 eV). Calculated and experimental ionisation rates agree excellently over a range of parameters which reaches far beyond the immediate vicinity of the threshold, where the Wannier threshold law (2) applies (cf. the dashed line in Fig. 4). We can assume that both the classical and the collinear approximations work excellently in this range, which is indicated by the thick long dashed lines in Figs 2*a* and 2*b*. It is always difficult to verify an analytical threshold law on the basis of numerical results in the near threshold region, but it does seem reasonable to assume that the good agreement of Fig. 4 is maintained when we approach the threshold $E \to 0$ while keeping the initial binding energy of the target fixed at $E_\mathrm{b} = \frac{1}{2}$, which corresponds to continuing to the origin on the appropriate half-parabola in Fig. 2*b*.

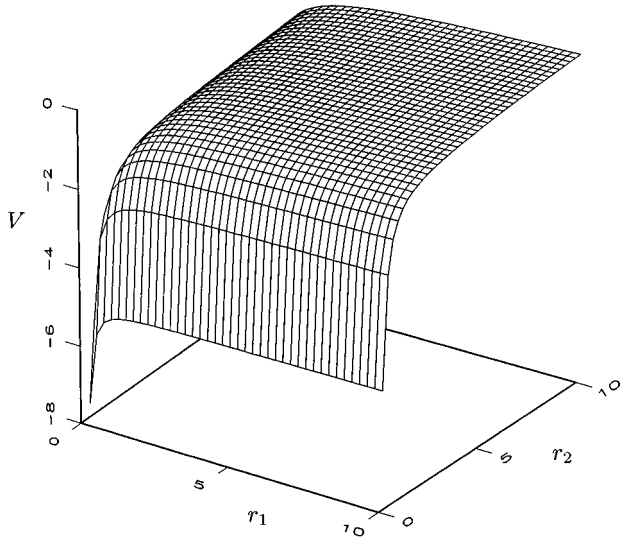

Fig. 3. The potential (13) for $Z = 1$.

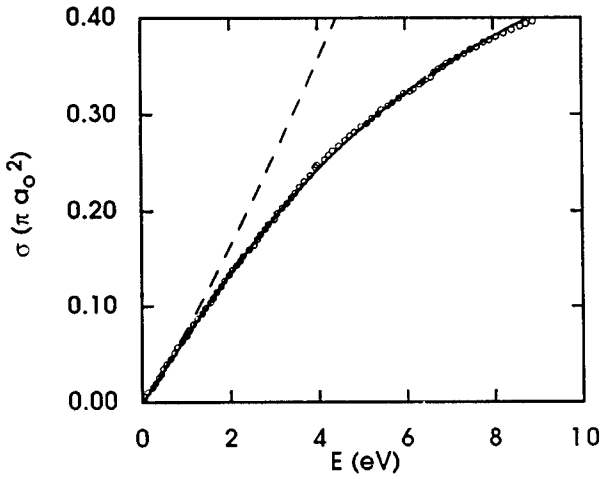

Fig. 4. Total ionisation cross sections for the reaction (1). The circles are the experimental data from McGowan and Clarke (1968), the solid line is the classical ionisation probability calculated in the collinear model (13) and scaled to agree with the data at one point (5·84 eV). The dashed line shows the proportionality to $E^{1\cdot127}$ according to Wannier's threshold law (2). [From Rost (1998).]

There are, however, situations where the behaviour of the quantum mechanical ionisation cross section for $E \to 0$ at fixed E_b differs significantly from the classical result. Such cases are the subject of the next two sections.

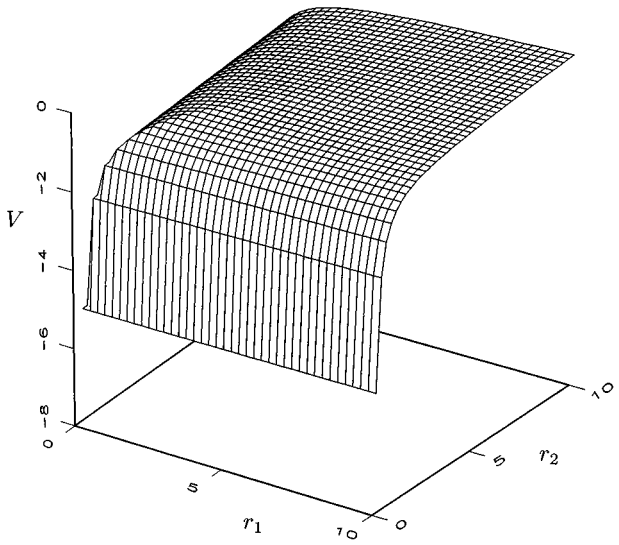

Fig. 5. The potential (14) for $Z = 1$.

4. The *s*-wave Model

A drastic simplification of the problem of two electrons in the field of an atomic nucleus is achieved by assuming spherical symmetry of each electron's wave function. Like the collinear model (13), this '*s*-wave model' has two variables, viz. the radial distances r_1 and r_2 of the spherical electrons from the (infinitely heavy) nucleus, but the potential now is

$$V_{\rm SW}(r_1, r_2) = -\frac{Z}{r_1} - \frac{Z}{r_2} + \frac{1}{r_>}\,, \tag{14}$$

where $r_>$ is the larger of the two radii, r_1 and r_2. It is illustrated in Fig. 5 for the case of a hydrogen target ($Z = 1$). The *s*-wave model implies a spherical world with one (radial) dimension, and this is different to the picture developed by Temkin (1962) and Poet (1978, 1980, 1981) where the concept of three-dimensional spatial variables is retained, but the electron–electron interaction is restricted to single-electron *s* waves, so the potential also has the form (14). All nonvanishing matrix elements of the interaction are the same in both models, but in the Temkin–Poet model there is an ionisation cross section with the dimensions of an area, as in the real case. The ionisation probability $\sigma^{\rm SW}$ of the *s*-wave model is related to the ionisation cross section $\sigma^{\rm TP}$ of the Temkin–Poet model by (Ihra *et al.* 1995)

$$\sigma^{\rm TP}(E) = \frac{\pi}{k^2}\sigma^{\rm SW}(E) = \frac{\pi/2}{E + E_{\rm b}}\sigma^{\rm SW}(E)\,, \tag{15}$$

where k is the wave number of the projectile electron, $E_{\rm inc} = k^2/2$ (in atomic units). The factor in front of $\sigma^{\rm SW}$ in (15) is essentially the area occupied by the

zero angular momentum component of the incoming wave front, and it expresses the decrease of the relative contribution of this s wave to the incoming plane wave as the energy $E_{\rm inc}$ of the projectile electron increases.

The s-wave model is unrealistic, because it ignores all angular degrees of freedom. It does, however, in the radial degrees of freedom, retain the effects of long-range Coulomb interactions and electron correlations. It is probably the simplest model where these effects can be investigated, and it has recently become a rather popular and widely studied system (Ihra *et al.* 1995, 1997*a*; Handke *et al.* 1993*a*, 1993*b*; Bray and Stelbovics 1994; Rudge 1996; Macek and Ihra 1997; Scott *et al.* 1997; Robicheaux *et al.* 1997). The quantum mechanical ionisation probabilities were obtained by Ihra *et al.* (1995) using a time-dependent approach, and the equivalent ionisation cross sections of the Temkin–Poet model have been calculated by Bray and Stelbovics (1994) using the convergent close coupling method. At this point it is worth mentioning that the s-wave model, as unrealistic as it may be, does rather accurately reproduce the energy dependence of the experimental integrated cross section for ionisation of hydrogen by electron impact. This is demonstrated in Fig. 6 showing the calculated ionisation probability from Ihra *et al.* (1995), which was scaled to agree with the experimental cross section at the maximum. The good agreement seems to indicate that the integrated cross sections are rather insensitive to the effects of angular correlations, which are completely absent in the s-wave model. For comparison, the short dashed line in Fig. 6 shows the ionisation cross section $\sigma^{\rm TP}$ obtained in the Temkin–Poet model (Bray and Stelbovics 1994), which is of course too small in comparison with experiment, because it only includes the contribution of the s waves. For a fair comparison with the solid curve in Fig. 6 we include a rescaled version of $\sigma^{\rm TP}$ (long dashed line) which reproduces the correct height at maximum. Note that, even after rescaling, $\sigma^{\rm TP}$ differs strongly from the experimental cross section (Shah *et al.* 1987), because the factor $\frac{1}{2}\pi/(E+E_{\rm b})$ exaggerates the fall-off towards higher energies, see equation (15).

The difference between the one-dimensional picture (s-wave model) and the three-dimensional picture (Temkin–Poet model) based on the potential (14) is not important when studying the threshold behaviour of the ionisation probability (cross section) at fixed initial binding energy $E_{\rm b}$, because the prefactor proportional to $1/(E+E_{\rm b})$ in (15) remains finite at $E=0$. Note, however, that for fixed scaled energy (7) we have $E+E_{\rm b}=E(1+\varepsilon)/\varepsilon$, so the relation (15) can be written as

$$\sigma^{\rm TP}(E)=\frac{\varepsilon\,\pi/2}{E(1+\varepsilon)}\,\sigma^{\rm SW}(E)\,, \tag{16}$$

and the threshold behaviour does differ by one power of E in the s-wave and the Temkin–Poet pictures.

The classical s-wave model is naturally defined as the classical one-dimensional two-particle system with the potential (14). It is not so clear that a classical version of the Temkin–Poet model can be defined consistently. If, for example, the cross sections of a classical Temkin–Poet model were related to that of the classical s-wave model via equation (15), then it would violate the classical scaling rules, because the factor $\frac{1}{2}\pi/(E+E_{\rm b})$ is not just a function of the scaled energy.

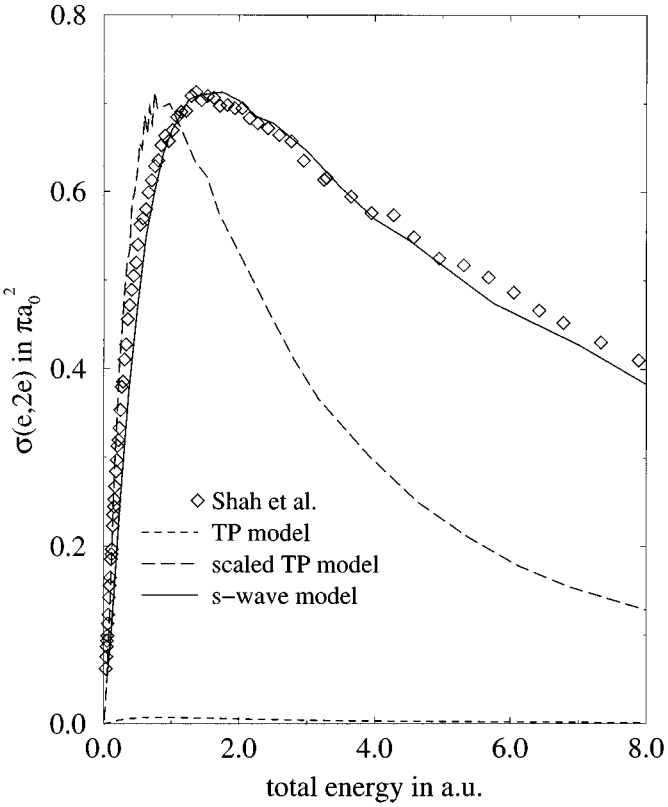

Fig. 6. Total ionisation cross sections for the reaction (1). The diamonds are the experimental data from Shah *et al.* (1987), the solid line is the quantum mechanical ionisation probability calculated in the *s*-wave model (14) and scaled to agree with the data at the maximum. The short dashed line is the ionisation cross section (15) according to the Temkin–Poet model, and the long dashed line is obtained by scaling this cross section to have the correct height at the maximum.

The classical ionisation probability in the *s*-wave model, $\sigma_{\rm cl}^{\rm SW}(E)$, was calculated by Handke *et al.* (1993*b*), and it has the interesting feature that it vanishes in a finite range of scaled energies, because all trajectories at these scaled energies fall back into the regime where one electron is bound. The energy range where this occurs defines a dynamical ionisation threshold below which ionisation is forbidden classically. The dynamical threshold is determined by a transcendental equation involving the nuclear charge Z (Handke *et al.* 1993*b*); for hydrogen ($Z = 1$) it is at $\varepsilon = \frac{1}{3}$, i.e.

$$\sigma_{\rm cl}(\varepsilon) = 0 \quad \text{for} \quad \varepsilon = E/E_{\rm b} \leq \tfrac{1}{3}\,. \tag{17}$$

The region above threshold where ionisation is forbidden in the classical *s*-wave model is bounded by the thin dashed lines in Figs 2*a* and 2*b*.

So far, the only analytical analysis of the quantum mechanical threshold behaviour in the *s*-wave model is based on a recently proposed semiclassical

theory of ionisation due to Macek and Ovchinnikov (1996). It is formulated in terms of the hyperspherical representation of the electron–nucleus separations, $R = \sqrt{r_1^2 + r_2^2}$, $\alpha = \arctan(r_2/r_1)$, so the potential energy of the two electrons in the field of the nucleus is

$$V(R, \alpha, \ldots) = \frac{C(\alpha, \ldots)}{R}\,, \tag{18}$$

and its dependence on the angular degrees of freedom and on the hyperangle α is contained in the function C. Both for the collinear model (13) and for the s-wave model (14), the only variable besides the hyperradius R is α. For the collinear model we have

$$\begin{aligned} C_{\mathrm{COL}}(\alpha) = & -\frac{Z}{\cos\alpha} - \frac{Z}{\sin\alpha} + \frac{1}{\sqrt{1+\sin 2\alpha}} \\ & \approx -\frac{4Z-1}{\sqrt{2}} - \frac{12Z-1}{2\sqrt{2}}\left(\alpha - \frac{\pi}{4}\right)^2 \quad \text{for} \quad \alpha \approx \pi/4\,. \end{aligned} \tag{19}$$

For the s-wave model we have,

$$\begin{aligned} C_{\mathrm{SW}}(\alpha) = & \begin{cases} -Z/\sin\alpha & \text{for} \quad \alpha < \pi/4 \\ -Z/\cos\alpha & \text{for} \quad \alpha > \pi/4 \end{cases}\,, \\ & \approx -Z\sqrt{2} - Z\sqrt{2}\left|\alpha - \frac{\pi}{4}\right| \quad \text{for} \quad \alpha \approx \pi/4\,. \end{aligned} \tag{20}$$

The lower lines in (19) and (20) represent the expansion around the 'Wannier ridge' $r_1 = r_2$ corresponding to $\alpha = \pi/4$.

In its simplest adiabatic form, the theory of Macek and Ovchinnikov describes the outgoing electrons via a WKB-type wave function. For the collinear or the s-wave model (Macek and Ihra 1997) it has the form

$$\Psi(R, \alpha) = \frac{\psi(R)}{\sqrt{R}}\phi_R(\alpha)\,, \quad \psi(R) = \frac{1}{\sqrt{K(R)}}\exp\left[\mathrm{i}\int_{R_0}^{R} K(R')\,dR'\right]. \tag{21}$$

The hyperradial momentum $K(R)$ is related to the available kinetic energy as a function of R; this is determined by the potential energy along the Wannier ridge, $r_1 = r_2$, and the energy of motion in the hyperangle degree of freedom, which is contained in the hyperangle wave function ϕ_R and depends on R as a parameter. In the Macek and Ovchinnikov theory, the hyperradius R is not restricted to the positive real axis, and the hyperangle wave function ϕ_R for large *negative* R is taken to be the ground state in the (binding) potential, obtained via (18) from the lower lines in (19) (collinear model) or in (20) (s-wave model). Analytic continuation to large positive values of R leads to a complex energy of the hyperangle wave function and to a complex hyperradial momentum

$K(R)$, and the imaginary part of $K(R)$ is a key to describing the near threshold behaviour of the ionisation current associated with the wave function (21).

Both for the full three-dimensional case (Macek and Ovchinnikov 1996) and for the collinear model (Macek and Ihra 1997) this theory yields a power law as in (2), but with a slightly modified exponent ν_{MO}:

$$\nu_{\mathrm{MO}} = \tfrac{1}{4}\left(\sqrt{\frac{96Z-8}{4Z-1}} - 1\right). \tag{22}$$

The exponent ν_{MO} is close to, but not equal to the Wannier exponent ν_{W}; in particular, it does not converge to unity as expected (Friedrich 1998*b*) for $Z \to \infty$.

The theory of Macek and Ovchinnikov was applied to the s-wave model by Macek and Ihra (1997) and by Ihra *et al.* (1997*a*), and it predicts an exponential supression of the quantum mechanical ionisation cross section as $E \to 0$ for fixed E_{b}. For hydrogen ($Z = 1$) the prediction is

$$\sigma_{\mathrm{qm}}^{\mathrm{SW}}(E) \propto \exp\left(-aE^{-1/6} + bE^{\frac{1}{6}}\right), \tag{23}$$

with $a = 6{\cdot}870$ and $b = 2{\cdot}770$ (Ihra *et al.* 1997*a*).

The constants a and b appearing in the threshold law (23) (Macek and Ihra 1997; Ihra *et al.* 1997*a*) were derived on the basis of an Airy function for the hyperangle motion, as this is the ground state wave function in the binding (for negative R) linear potential derived from (18) and the lower line of (20). Improvements are conceivable based on better approximations of the hyperangle potential $C(\alpha)/R$ ($R < 0$, fixed), e.g. by a Coulomb potential reproducing the correct $1/\alpha$-behaviour near the axis $\alpha = 0$. If the resulting ground state wave function is again approximated by an Airy function, the exponent $aE^{-1/6} + bE^{\frac{1}{6}}$ in (23) keeps its structure, but the constant b is changed when the calculation is based on the more realistic slope of the Coulomb potential at the turning point. In a more sophisticated treatment beyond the Airy function approximation, it is not obvious that Macek and Ovchinnikov's theory will give a result of the form (23).

The threshold behaviour of numerically calculated ionisation cross sections $\sigma_{\mathrm{qm}}^{\mathrm{TP}}(E, E_{\mathrm{b}} = \frac{1}{2})$ has been studied by Scott *et al.* (1997), who found that the expression (23) fits the calculated data well when choosing $a = 11{\cdot}916$ (and $b = 0$), which is close to being the square of the function based on $a = 6{\cdot}870$ (see Macek and Ihra 1997; Ihra *et al.* 1997*a*). The fit by Scott *et al.* (1997) was also hardly distinguishable from a fit to a quadratic energy dependence, which is favoured by Rudge (1996) and Robicheaux *et al.* (1997). Exponential suppression of quantum mechanical near threshold ionisation seems plausible, considering that ionisation is forbidden classically in the finite range of energies, $E/E_{\mathrm{b}} < \frac{1}{3}$ (for $Z = 1$) (Handke *et al.* 1993*b*). In this energy range there are no (real) classical paths contributing to the semiclassical transition amplitude and ionisation can only proceed via a form of tunnelling. In a recent fit of numerically calculated ionisation cross sections to the expression $\exp(-aE^{-1/6})$, Miyashita *et al.* (1999) obtain values of 6.65 and 6.75 for a, which is quite close to the prediction of Ihra *et al.*

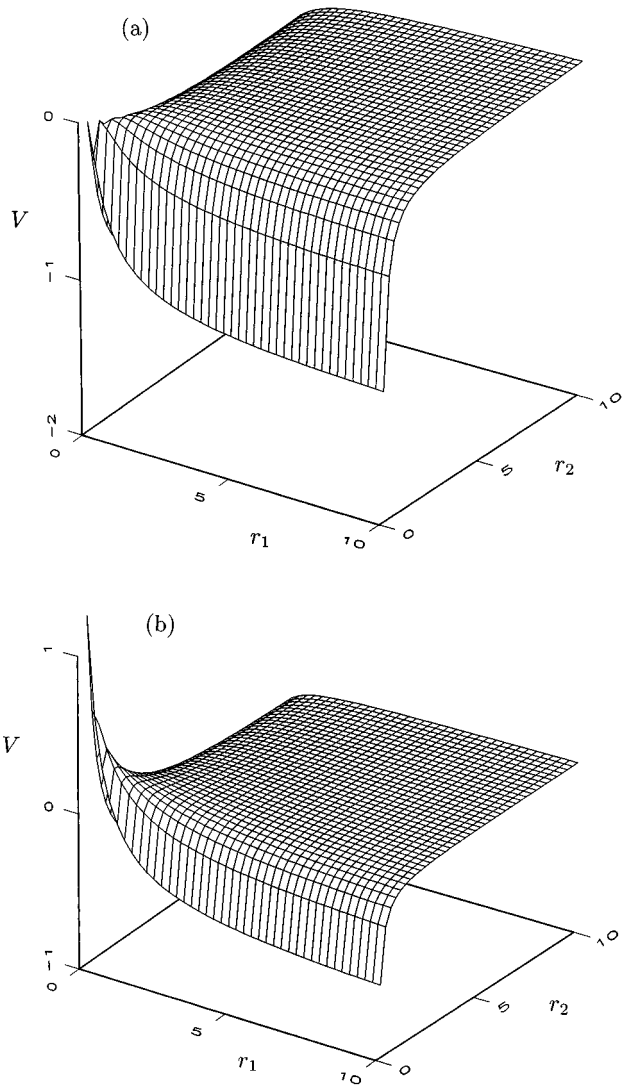

Fig. 7. The potential (13) (*a*) for $Z = \frac{1}{4}$ and (*b*) for $Z = \frac{1}{8}$.

5. The Case $Z = \frac{1}{4}$

The exponent ν_{W} in Wannier's threshold law (2) diverges when the nuclear charge approaches $\frac{1}{4}$. Such a situation effectively corresponds to a system in which the electrons in (1) are replaced by other particles with an equal charge which is four times the magnitude and of opposite sign as the charge of the 'nucleus', e.g. two beryllium nuclei in the field of a singly charged heavy negative ion. The breakdown of the traditional Wannier treatment in this case can already be understood in the simple collinear model (18), (19). For $Z = \frac{1}{4}$, the constant term in the lower line of (19) is zero, so the potential (18) vanishes on the

'Wannier ridge', $\alpha = \pi/4$ (corresponding to $r_1 = r_2$), see Fig. 7*a*. For $Z < \frac{1}{4}$, the constant term in (19) is positive so there is a *repulsive* Coulomb potential on the 'Wannier ridge', see Fig. 7*b*. For ionisation to take place, a trajectory now has to reach the flat part of the potential shown in Fig. 7*b* by moving around or tunnelling through the repulsive Coulomb barrier without getting caught in the deep side ditches, $\alpha \approx 0$ or $\alpha \approx \pi/2$, which correspond to direct and exchange scattering respectively.

Ihra *et al.* (1997*b*) have applied Macek and Ovchinnikov's theory to the case $Z = \frac{1}{4}$, and, taking the limit $E \to 0$ for fixed initial binding energy E_b, they obtained an exponential threshold law

$$\sigma(E) \propto E^{-1/6} \exp\left[-\kappa E^{-1/6}\right], \tag{24}$$

with an analytically given constant κ whose numerical value is $\approx 6{\cdot}758$. The term proportional to $E^{-1/6}$ in the exponent can be understood by a simple scaling argument in this case. The term proportional to $1/R$ in the potential (18), (19) vanishes for $\alpha = \pi/4$. The (complex) zero-point energy in the hyperangle is proportional to $R^{-3/2}$ and the leading contributions to the hyperradial momentum $K(R)$ are proportional to $R^{-3/4}$ when the total energy E can be neglected. Thus the integral in (21) is proportional to the fourth root of its upper limit R_l, and this in turn is chosen as the boundary of the region where the total energy is still negligible compared to the zero-point energy mentioned above, $R_\mathrm{l}^{-3/2} \approx E$, which implies $R_\mathrm{l}^{\frac{1}{4}} \approx E^{-1/6}$, and this is the power of E appearing in the exponent (see Ihra *et al.* 1997*b*).

When the expressions derived from the Macek and Ovchinnikov theory are analysed for fixed values of the scaled energy (7), we can use the relations

$$E \approx \text{const.}E_\mathrm{b} \equiv \frac{\text{const.}'}{R_0} \overset{R_0 \gg 1}{\gg} \frac{\text{const.}'}{R_0^{3/2}}, \tag{25}$$

where R_0 is some length characteristic of the spatial extension of the initial bound state of the target. Taking the classical limit, $E \to 0$, $E_\mathrm{b} \to 0$ for fixed E/E_b, implies $R_0 \to \infty$, so the total energy E can be assumed to be much larger than the contributions of the potential ($\propto R^{-3/2}$) to the hyperradial momentum $K(R)$ in the whole range of the integral in (21). On the basis of these inequalities, Ihra *et al.* (1997*b*) derived the following near threshold behaviour ($\varepsilon = E/E_\mathrm{b} \to 0$) for the ionisation probability in the classical limit:

$$\sigma_\mathrm{cl}(\varepsilon) \propto \exp\left(-\frac{\lambda}{\sqrt{\varepsilon}}\right). \tag{26}$$

Classical ionisation probabilities in the collinear model have been obtained by Chocian *et al.* (1998) by numerically solving the classical equations of motion. For $Z = \frac{1}{4}$ the best fit to the form $\sigma_\mathrm{cl} \propto \exp(-\lambda/\sqrt{\varepsilon})$ was obtained for $\lambda = 1{\cdot}7288$. Dimitrijević *et al.* (1994) performed classical trajectory calculations for $Z = \frac{1}{4}$ in three-dimensional space and fitted calculated ionisation cross sections to the

ansatz $\sigma_{\rm cl} \propto \exp(-\lambda/\sqrt{\varepsilon - \varepsilon_0})$. Their best fit was for $\lambda \approx 1{\cdot}868$, and they also found that the fit could be improved by introducing a nonvanishing threshold ε_0 of the order of 10^{-3}. This would correspond to a small range of energies, where ionisation is strictly forbidden classically, and was interpreted by Dimitrijević *et al.* (1994) as a consequence of the repulsive Coulomb barrier facing the incoming electron in the initial stages of the collision. No evidence for such a strictly forbidden region above threshold was seen in the (one-dimensional) calculations of Chocian *et al.* (1998). In both cases (Chocian *et al.* 1998; Dimitrijević *et al.* 1994), the numerical calculations appear to be accurate enough to rule out a power-law behaviour of the near threshold ($\varepsilon \to 0$) ionisation cross section $\sigma_{\rm cl}$, see e.g. Fig. 8.

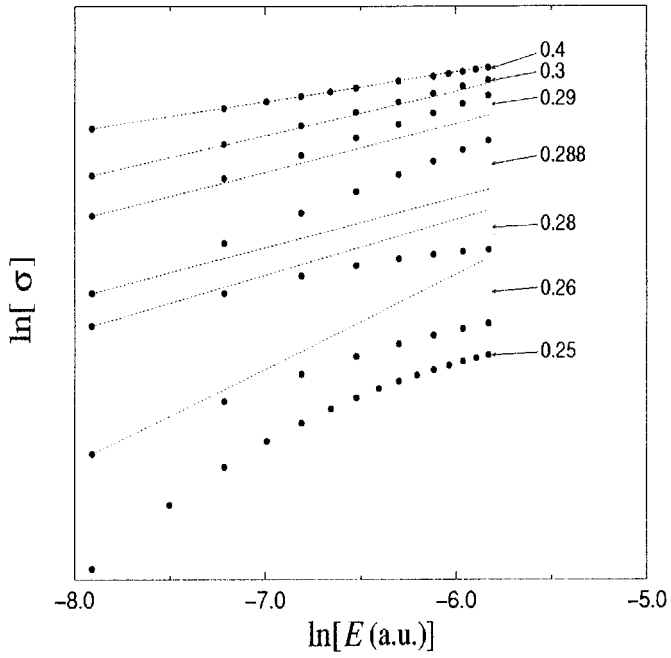

Fig. 8. Numerically calculated classical total ionisation probability in the collinear model (13) for various nuclear charges Z in the vicinity of $Z = \frac{1}{4}$. For $Z > \frac{1}{4}$ the straight dotted lines correspond to the power law (2). [From Chocian *et al.* (1998).]

For $Z = \frac{1}{4}$, ionisation is apparently not forbidden classically above the threshold, but it is strongly inhibited. The damping of the *classical* ionisation probability as $\exp(-c/\sqrt{\varepsilon})$ is actually what one expects for the *quantum mechanical* tunnelling probability near the base of a Coulombic potential barrier. The quantum mechanical cross sections derived by Ihra *et al.* (1997*b*) show, as expected, a weaker damping, with the power $E^{-1/6}$ in the exponent rather than $E^{-1/2}$. A more detailed analysis of the dependence of the cross section on the initial binding energy should make it possible to follow the transition from the quantum case (fixed $E_{\rm b}$, $E \to 0$) to the classical limit (fixed $E/E_{\rm b}$, $E \to 0$).

6. Summary

The classical dynamics of a collision process, in which a projectile collides with a target of initial binding energy E_b, depends only on the scaled energy $\varepsilon = E/E_\mathrm{b}$ if the potential energy is a homogeneous function of the coordinates. The quantum mechanical properties of such a system depend on E and E_b independently. For a system of particles interacting exclusively via Coulomb forces, the square root of the total energy E plays the role of an effective Planck constant and the classical (semiclassical) limit is reached for fixed values of the scaled energy ε as $\sqrt{E} \equiv \hbar' \to 0$. Quantum mechanical ionisation cross sections $\sigma_\mathrm{qm}(E, E_\mathrm{b}) \equiv \sigma_\mathrm{qm}(\varepsilon, \hbar')$ are usually calculated or measured for fixed initial binding energies E_b, and the threshold behaviour obtained for $E \to 0$ can differ from the classical threshold behaviour, $\sigma_\mathrm{cl}(\varepsilon)$. The limiting behaviour near the origin in Fig. 2*b* depends on whether it is approached along the ordinate $\hbar' = 0$ or along a half-parabola $E_\mathrm{b} = \mathrm{const}$. If we first calculate, in analogy to scaled energy spectroscopy, $\sigma_\mathrm{qm}(E, E_\mathrm{b})$ for fixed E/E_b and then take the limit $\sqrt{E} \equiv \hbar' \to 0$, this should always lead to the classical (semiclassical) result.

In the traditional Wannier situation, near threshold ionisation is described via allowed classical trajectories, and an estimate of the dependence of the available phase space leads to a simple power law for the near threshold behaviour, see e.g. equation (2). In such a power law, the dependence on the initial binding energy affects only the proportionality constant and not the shape of the ionisation cross section. The situation changes when near threshold ionisation is classically forbidden, as in the *s*-wave model, or strongly inhibited, as in the case of two light particles whose charge is four times as large and of opposite sign as the heavy central particle, a situation which effectively corresponds to nuclear charge $Z = \frac{1}{4}$ in the electron–nucleus–electron picture. In both cases, recent theoretical studies predict an exponentially damped (quantum mechanical) ionisation cross section near threshold.

For a more complete understanding of the ionisation process in the interesting 'non-Wannier' situations, it is highly desirable to study in more detail the dependence of the quantum mechanical ionisation cross sections on the initial binding energy, as this should make a direct connection to the classical results possible, at least in the near threshold regime. This will require more detailed descriptions of the interaction of the electrons in the early stages of the collision.

Acknowledgments

It is a pleasure to thank Andris T. Stelbovics for helpful and enlightening discussions. This work was supported by the Deutsche Forschungsgemeinschaft, Az: Fr-591/7–2.

References

Bray, I., and Stelbovics, A. T. (1993). *Phys. Rev. Lett.* **70**, 746.
Bray, I., and Stelbovics, A. T. (1994). *At. Data Nucl. Dat. Tables* **58**, 67.
Chocian, P., Ihra, W., and O'Mahony, P. F. (1998). *Phys. Rev.* A **57**, 3583.
Dimitrijević, M. S., Grujić, P. V., and Simonović, N. S. (1994). *J. Phys.* B **27**, 5717.
Feagin, J. M. (1984). *J. Phys.* B **17**, 2433.
Friedrich, H. (1998*a*). *In* 'Atoms and Molecules in Strong External Fields' (Eds P. Schmelcher and W. Schweizer), p. 153 (Plenum: New York).

Friedrich, H. (1998*b*). 'Theoretical Atomic Physics', 2nd edn (Springer: Berlin, Heidelberg).
Friedrich, H., and Eckhardt, B. (Eds) (1997). 'Classical, Semiclassical and Quantum Dynamics in Atoms', Lecture Notes in Physics, Vol. 485 (Springer: Berlin, Heidelberg).
Handke, G., Draeger, M., and Friedrich, H. (1993*a*). *Physica* A **197**, 113.
Handke, G., Draeger, M., Ihra, W., and Friedrich, H. (1993*b*). *Phys. Rev.* A **48**, 3699.
Ihra, W., Draeger, M., Handke, G., and Friedrich, H. (1995). *Phys. Rev.* A **52**, 3752.
Ihra, W., Mota-Furtado, F., O'Mahony, P. F., and Macek, J. H. (1997*a*). *Phys. Rev.* A **55**, 3250.
Ihra, W., Mota-Furtado, F., and O'Mahony, P. F. (1997*b*). *Phys. Rev.* A **55**, 4263.
Kuchiev, M. Y., and Ostrovsky, V. N. (1998). *Phys. Rev.* A **58**, 321.
Landau, L. D., and Lifshitz, E. M. (1971). 'Course of Theoretical Physics', Vol. 1, 'Mechanics' (Addison–Wesley: Reading, MA).
McGowan, J. W., and Clarke, E. M. (1968). *Phys. Rev.* **167**, 43.
Macek, J. H., and Ihra, W. (1997) *Phys. Rev.* A **55**, 2024.
Macek, J. H., and Ovchinnikov, S. Y. (1996). *Phys. Rev.* A **54**, 544.
Miyashita, N., Kato, D., and Watanabe, S. (1999). *Phys. Rev.* A **59**, 4385.
Poet, R. (1978). *J. Phys.* B **11**, 3081.
Poet, R. (1980). *J. Phys.* B **13**, 2995.
Poet, R. (1981). *J. Phys.* B **14**, 91.
Rau, A. R. P. (1971). *Phys. Rev.* A **4**, 207.
Robicheaux, F., Pindzola, M. S., and Plante, D. R. (1997). *Phys. Rev.* A **55**, 3573.
Rost, J. M. (1994). *Phys. Rev. Lett.* **72**, 1998.
Rost, J. M. (1998). *Phys. Rep.* **297**, 271.
Rudge, M. R. H. (1996). *J. Phys.* B **29**, 4689.
Schmelcher, P., and Schweizer, W. (Eds) (1998). 'Atoms and Molecules in Strong External Fields' (Plenum: New York).
Scott, M. P., Burke, P. G., Bartschat, K., and Bray, I. (1997). *J. Phys.* B **30**, L309.
Shah, M. B., Elliott, D. S., and Gilbody, H. B. (1987). *J. Phys.* B **20**, 3501.
Temkin, A. (1962). *Phys. Rev.* **126**, 130.
Temkin, A. (1991). *J. Phys.* B **24**, 2147.
Wannier, G. H. (1953). *Phys. Rev.* **90**, 817.

Manuscript received 5 November 1998, accepted 1 February 1999